Fish and Shellfish Immunology 92 (2019) 655–666

Contents lists available at ScienceDirect

Fish and Shellfish Immunology

journal homepage: www.elsevier.com/locate/fsi

Full length article

Molecular characterization and expression analysis of rockfish (*Sebastes schlegelii*) viperin, and its ability to enervate RNA virus transcription and replication *in vitro*

K.A.S.N. Shanaka[a], M.D. Neranjan Tharuka[a,b], Thanthrige Thiunuwan Priyathilaka[a], Jehee Lee[a,b,*]

[a] Department of Marine Life Sciences & Fish Vaccine Research Center, Jeju National University, Jeju Self-Governing Province, 63243, Republic of Korea
[b] Marine Science Institute, Jeju National University, Jeju Self-Governing Province, 63333, Republic of Korea

ARTICLE INFO

Keywords:
Sebastes schlegelii
Viperin
Antiviral protein
Immune challenge
Subcellular localization
mRNA expression
Innate immunity

ABSTRACT

Viperin, also known as RSAD2 (Radical S-adenosyl methionine domain containing 2), is an interferon-induced endoplasmic reticulum-associated antiviral protein. Previous studies have shown that viperin levels are elevated in the presence of viral RNA, but it has rarely been characterized in marine organisms. This study was designed to functionally characterize rockfish viperin (*SsVip*), to examine the effects of different immune stimulants on its expression, and to determine its subcellular localization. SsVip is a 349 amino acid protein with a predicted molecular mass of 40.24 kDa. It contains an S-adenosyl L-methionine binding conserved domain with a CNYK-CGFC sequence. Unchallenged tissue expression analysis using quantitative real time PCR (qPCR) revealed *SsVip* expression to be the highest in the blood, followed by the spleen. When challenged with poly I:C, *SsVip* was upregulated by approximately 60-fold in the blood after 24 h, and approximately 50-fold in the spleen after 12 h. Notable upregulation was detected throughout the poly I:C challenge experiment in both tissues. Significant expression of *SsVip* was detected in the blood following *Streptococcus iniae* and lipopolysaccharide challenge, and viral hemorrhagic septicemia virus (VHSV) gene transcription was significantly downregulated during SsVip overexpression. Furthermore, cell viability assay and virus titer quantification with the presence of SsVip revealed a significant reduction in virus replication. As with previously identified viperin counterparts, SsVip was localized in the endoplasmic reticulum. Our findings show that SsVip is an antiviral protein crucial to innate immune defense.

1. Introduction

Upon viral infection a dedicated set of proteins named interferons (IFNs) [1], which form part of the innate immune system, induce transcription of interferon regulated genes (IRGs) [2]. Viperin is an endoplasmic reticulum-associated IRG in animals, whose expression is induced by both type I and II IFNs [3]. Although this protein specifically acts on RNA viruses [4], it has also been shown to elicit a broad range of responses against DNA viruses and other immune stimuli, including bacterial pathogens and endotoxins [5].

Viperin is a member of the radical SAM superfamily of enzymes, which possess a 4Fe–4S cluster in their catalytic center [5]. A tri-cysteine CxxxCxxC motif is a universal feature among these enzymes, and plays an important role in coordinating the 4Fe–4S cluster [6]. Viperin has three main domains, namely an N-terminal signal domain, a middle 4Fe–4S cluster binding catalytic domain, and a C-terminal domain [4]. The N-terminal amphipathic signal helix plays a vital role in localizing viperin to the endoplasmic reticulum (ER) membrane [7].

To explain viperin expression, interferon-dependent and independent pathways have been proposed [8]. In the interferon-dependent pathway, antigens such as lipopolysaccharide (LPS), double standard RNA (dsRNA), and polyinosinic:polycytidylic acid (poly I:C) bind to activate Toll-like receptors (TLR), cytosolic retinoic acid-inducible gene I (RIG-I) like receptors (RLRs), and cytosolic DNA sensors [9]. Activated receptors subsequently activate interferon regulatory factors (IRFs) IRF 3 and IRF 7, resulting in the production of type I IFN which is believed to act in either an autocrine or paracrine manner [3]. IFNs binding to cell surface type I interferon receptors induces the formation

* Corresponding author. Marine Molecular Genetics Lab, Department of Marine Life Sciences, College of Ocean Science, Jeju National University, 66 Jejudaehakno, Ara-Dong, Jeju, 690-756, Republic of Korea.
E-mail address: jehee@jejunu.ac.kr (J. Lee).

https://doi.org/10.1016/j.fsi.2019.06.015
Received 11 March 2019; Received in revised form 4 June 2019; Accepted 9 June 2019
Available online 25 June 2019

of interferon stimulated gene (ISG) factor 3 (ISGF-3), which is capable of binding with the viperin promotor [10].

In the interferon-independent mechanism, viperin upregulation takes place through IRF1 (interferon regulatory factor 1) and IRF3 [3]. After stimulation with dsRNA, cytosolic RLRs, which are a group of soluble RNA helicases [11], interact with an adaptor protein named mitochondria-associated adaptor molecule (MAVS) [12]. MAVS binds to RLR and promotes the activation of various IRFs, which induce expression of ISGs, and of viperin [13].

Number of discrete mechanisms have been developed to explain viperin's antiviral effect [5,8,14–16]. One mechanism is inhibition of virus through formation of unstable lipid rafts [15]. Viruses depend on lipid rafts for entry, assembly, and release by budding [17]. In this mechanism viperin interacts with farnesyl pyrophosphate synthase (FPPS), which is involved in the synthesis of precursors for important cell membrane isoprenoids such as sterols [18]. Suppression by viperin results in the formation of unstable lipid rafts, which viruses are unable to use for completion of their life cycle [19]. However, accumulating information suggests that viperin is unable to interact directly with FPPS [20]. A more comprehensive mechanism has recently been proposed to explain viperin's mode of action, in which viperin radically generates 3′-deoxy-3′,4′didehydro-CTP (ddhCTP) from the available CTP pool, leading to the inhibition of viral RNA-dependent RNA polymerase (RdRp) through a chain termination mechanism [21]. Furthermore, in virus infected cells, generated ddhCTP acts as regulatory molecule inciting the cellular antiviral mode [21].

Human viperin was initially identified in human cytomegalovirus (HCMV) infected cells [22]. In fishes viperin was initially identified in VHSV-infected rainbow trout (*Oncorhynchus mykiss*) [23]. Mammalian viperin is an extensively studied protein compared to its piscine counterpart. Several studies on fishes have been performed, which have included tilapia (*Oreochromis niloticus*) [24], red drum (*Sciaenops ocellatus*) [25], mandarin fish (*Siniperca chuatsi*) [26], Atlantic salmon (*Salmo salar*) [27], crucian carp (*Carassius auratus*) [28], rock bream (*Oplegnathus fasciatus*) [29], and seahorse (*Hippocampus abdominalis*) [30].

Rockfish (*Sebastes schlegelii*) is one of the most important fish species in South Korea, and the species has been used extensively in offshore mariculture [31]. Virus diseases among fishes can have devastating consequences, causing worldwide economic loses to fish farmers [32,33]. Therefore, studies on antiviral proteins are of paramount importance to future vaccination programs. Despite this, SsVip has not yet been studied. To address this research gap, we characterized SsVip in the present study, analyzing expression profiles of *SsVip* under immune challenge with LPS, poly (I:C), and *Streptococcus iniae* (*S. iniae*). Moreover, *SsVip* was transiently transfected into fathead minnow (FHM) cells to investigate its antiviral effects against VHSV. In addition, the SsVip ability to enhance cell viability under VHSV challenge was studied. Finally, subcellular localization of SsVip was examined.

2. Materials and methods

2.1. Identification of coding sequence of SsVip

The coding sequence of rockfish viperin *SsVip* was identified from a previously constructed rockfish transcriptome database [34] using the Basic Local Alignment Search Tool (BLAST) from the National Center for Biotechnology Information (NCBI) [35].

2.2. In silico analysis

The translated amino acid sequence of SsVip was obtained using Unipro UGENE (version 1.31.0) [36]. The molecular weight and isoelectric point of the protein were calculated using the ExPASy compute pI/Mw online tool [37]. A BLAST search was performed to identify viperin orthologues from other animals. Selected, previously characterized, orthologues were used to perform a multiple sequence alignment in ClustalW2 [38]. Pairwise sequence alignment was performed to disclose identity and similarity with other viperin orthologues using EMBOSS Needle [39]. Structural modeling was performed with SWISS-MODEL [40]. Surface modeling of SsVip was performed using UCSF Chimera (Version 1.13.1) [41]. N-terminal helix wheel simulations of the SsVip were carried out using the NetWheels online helical wheel projection tool (http://lbqp.unb.br/NetWheels). Phylogenetic tree construction was performed in MEGA software (Version 10.0.5) [42] using the neighbor-joining method, with a bootstrap value of 5000.

2.3. Rearing fish

Rockfish (Weight around 100 g) were obtained from the Marine Science Institute at Jeju National University, Jeju Self-Governing Province, Republic of Korea. Fish were visually inspected for morphological, physiological, and behavioral abnormalities. Any fish having such abnormalities were immediately discarded. Fish were adapted to laboratory conditions in aerated fresh seawater for two weeks (22 ± 1 °C, salinity 34% ± 1%, pH 7.6 ± 0.5) prior to experiments.

2.4. Challenge experiment and tissue sampling

In order to evaluate *SsVip* expression in different rockfish tissues, peripheral blood cells (PBCs), gills, liver, spleen, head kidney (H.Kidney), kidney, skin, muscle, heart, brain, testes, ovary and intestine organs/tissues were collected from three rockfish (approximately 100 g each). PBCs were separated from plasma by centrifugation (10 min at 3000 × *g*, 4 °C). To evaluate immune responses of *SsVip*, a time course experiment with immune stimulants including LPS from *Escherichia coli* (*E. coli* 055: B5, Sigma, USA), poly I:C (Sigma, USA) and *S. iniae* (provided by Department of Aqua life Medicine at Chonnam National University, Republic of Korea) was performed. The levels of the immune stimulants used for the study were as follows: 0.125 mg LPS, 0.15 mg poly I:C and 1×10^7 CFU/μL of *S. iniae*. Sterile phosphate buffered saline (PBS; pH 7.4) was used as the control for all tissue challenge experiments. Tissue samples including PBCs and spleen were obtained from three fish after 3, 6, 12, 24, 48, and 72 h post injection. Samples were then snap frozen in liquid nitrogen and stored −80 °C for further processing.

2.5. Construction of expression plasmids

To functionally evaluate *SsVip*, its coding DNA sequence (CDS) was cloned into pcDNA™3.1(+) (Invitrogen, USA). Two primers, VpCDNA-F and VpCDNA-R (Synthesized by Macrogen, Korea) (Table 1), harboring *BamH*I and *EcoR*I restriction sites, respectively, were designed. To determine subcellular localization, the *SsVip* CDS was cloned into pEGFPN1 (Clontech, USA). To accomplish this, a pair of primers, VpGEFP-F and VpGEFP-R (Synthesized by Macrogen, Korea), containing *EcoR*I and *BamH*I restriction sites, respectively, were designed separately. The *SsVip* CDS was amplified in a 50 μL reaction mixture containing 1 × Ex Taq buffer (TaKaRa, Japan), 5U of Ex Taq polymerase (TaKaRa, Japan), 8 μL of 2.5 mM dNTPs (TaKaRa, Japan), 50 pmol of each primer pair (VpCDNA-F/R or VpEGFP-F/R), and approximately 50 ng of cDNA, which was measured by UV spectroscopically (NanoDrop 2000C, Thermoscientific, USA). The PCR cycling profile included an initial single denaturation step of 94 °C for 1 min, 30 amplification cycles at 94 °C for 30 s, 58 °C for 30 s, and 72 °C for 45 s, and a final extension step of 72 °C for 5 min. PCR products were separated on a 1% agarose gel along with the 100 bp DNA ladder marker (MGmed, Korea). After 20 min gel electroporation (Mupid® exU, Japan), DNA was visualized using a UV illuminator (OPTINITY, Korea). The 1000 bp bands were purified using a gel purification kit (AccuPrep®, Bioneer, USA). Purified pcDNA™3.1(+) plasmids and PCR products were completely digested with BamHI (TaKaRa, Japan) followed by EcoRI (TaKaRa, Japan) restriction enzymes (37 °C, 3 h). Ligation of the digested products was performed using a DNA Ligation Mighty Mix kit (TaKaRa, Japan) at 16 °C for 30 min followed by overnight incubation at 4 °C. Ligated constructs were transformed into competent *E. coli* DH5α cells. Transformants were selected through

Table 1
Primers used in this study.

Primer	Purpose	Sequence (5′ to 3′)
SsVipF	qPCR forward	TGCCTCGTTCCTGAGTCCAATGA
SsVipR	qPCR Reverse	AAGGATGGACTTTGACGGGTCCT
VpCDNA-F	Viperin cloning into pcDNA 3.1(+)vector	GAGAGAggatccaccATGAAATTCTCCTCTGTGC
VpCDNA-R	Viperin cloning into pcDNA 3.1(+)vector	GAGAGAgaattcCCACTCCAGCTTCATGTCAGC
VpEGFP-F	Viperin cloning into pGEFPN1	GAGAGAgaattcaccATGAAATTCTCCTCTGTGC
VpEGFP-R	Viperin cloning into pGEFPN1	GAGAGAggatccCCACTCCAGCTTCATGTCAGC
GVHSVF	qPCR VHSV G protein forward	TACAACATCACCCTGCCCAACC
GVHSVR	qPCR VHSV G protein reverse	GACCACCCTGTGATCATGTGTCC
MVHSVF	qPCR VHSV M protein forward	CTGGTTCGCCTATTCCAGAGTGC
MVHSVR	qPCR VHSV M protein reverse	GGTCCAGGTAAGTGGCCTTTGC
NVHSVF	qPCR VHSV N protein forward	TGTCTCAGATCAGTGGGAAGTACGC
NVHSVR	qPCR VHSV N protein reverse	GGACCTCAGCGACAAGTTCGG
PVHSVF	qPCR VHSV P protein forward	CGACAACATACTCTCCATCC
PVHSVR	qPCR VHSV P protein reverse	CCAAGTGCTCTCTCATTCC
RdRpF	qPCR VHSV RdRp protein forward	CAAGTGCGGACACGATCAATCCC
RdRpR	qPCR VHSV RdRp protein reverse	TGAGGAAAGGGCAACCATTCGC
RfEFA-F	qPCR Internal control for rockfish forward	AACCTGACCACTGAGGTGAAGTCTG
RfEFA-R	qPCR Internal control for rockfish reverse	TCCTTGACGGACACGTTCTTGATGTT
FHMEf1α_qF	qPCR Internal control for FHM cells forward	GGCTGACTGTGCTGTGCTGAT
FHMEf1α_qR	qPCR Internal control for FHM cells reverse	GTGAAAGCCAGGAGGGCATGT

ampicillin (Sigma, USA) resistance or kanamycin (Sigma, USA) resistance. Putative constructs were validated by sequencing (Macrogen, Korea). Finally, plasmids were purified using a MIDI kit (Qiagen, USA) for FHM cell transfection.

2.6. Cell culture, VHSV

To evaluate viperin's effect on cell viability, its antiviral nature, and sub-cellular localization, pcDNA™3.1(+)*/SsVip* and pEGFPN1*/SsVip* were transfected into FHM cells. FHM cells were cultured at 20 °C in L-15 media (Sigma) supplemented with fetal bovine serum (FBS) 10%, penicillin 1%, and streptomycin 1%. Maintenance and propagation of VHSV was carried out as previously described [30].

2.7. Plasmid transfection and virus infection assay

To analyze alterations in VHSV gene expressions in the presence of SsVip, FHM cells were seeded in a six well plate (SPL life sciences, Korea) with each well containing approximately 1×10^5 cells. Cells were incubated 24 h at 20 °C prior to transfection to achieve approximately 80% of visual confluency (10 × 10 power, Leica Microsystems, Germany). The cells were then transiently transfected with 1 μg of pcDNA™3.1(+)*/SsVip* or empty pcDNA™3.1(+) vectors using X-tremeGENE™ 9 transfection reagent (Roche, USA). 24 h post transfection (p.t.), cells were treated with 0.01 multiplicity of infection (MOI) of VHSV (FWando05) [43] dissolved in L-15 growth medium (Sigma, USA). The resulting samples were divided into two groups which were incubated for 24 h or 48 h at 20 °C.

2.8. Total RNA extraction and cDNA synthesis

In the challenge experiment, total RNA was extracted from pooled tissue (50 mg each) samples from three different animals. In the viral RdRp attenuation assay, FHM cells were used for RNA extraction. Total RNA was extracted from tissues or cells using Tri Reagent™ (Sigma, USA), and purified with an RNeasy mini kit (Qiagen, USA). RNA quality was checked by electrophoresis, and its concentration was determined by UV spectroscopy (NanoDrop 2000C, Thermoscientific, USA). cDNA was synthesized using a PrimeScript™ cDNA synthesis kit (TaKaRa, Japan) and 2.5 μg of extracted RNA from each sample.

2.9. Quantitative real-time PCR (qPCR)

Primers for *in vivo* (SsVip) and *in vitro* (five VHSV genes: Nucleoprotein (NP) [AGS83377.1], phosphoprotein (PP) [AGS83378.1], matrix protein (MP) [AGS83379.1], glycoprotein (GP) [AGS83380.1], and RNA-dependent RNA polymerase (RdRp) [AGS83380.1]) qPCR were designed using the PrimerQuest online tool (https://sg.idtdna.com/PrimerQuest) (Table 1) according to "Minimum Information for Publication of Quantitative Real-Time PCR experiments (MIQE)" guidelines [44]. qPCR reactions were performed in triplicate in a reaction volume of 10 μL containing 3 μL of cDNA template, 0.4 μL of each qPCR primer (10 pmol/μL), 5.0 μL of 2 × SYBR® Premix Ex Taq™ (TaKaRa, Japan), and 1.2 μL of PCR-grade water. Reactions were run in a Real-Time system Thermal Cycler Dice™ system III TP950 (TaKaRa, Japan) under the following conditions: 95 °C for 10 s, followed by 45 cycles at 95 °C for 5 s, 60 °C for 10 s, and 72 °C for 20 s, and a final cycle at 95 °C for 5 s, 60 °C for 30 s, and 95 °C for 15 s. Rockfish elongation factor-1-alpha (*EF1α*, accession no. KF430623) and fathead minnow elongation factor-1 -alpha (*FHMEF1α*, accession no. AY643400) was used as internal controls for the *in vivo* and *in vitro* experiments, respectively (Table 1). Relative mRNA expression was analyzed by the Livak $2^{-\Delta\Delta CT}$ method [45].

2.10. Cell viability analysis through MTT assay

An MTT assay was performed to analyze the impact of SsVip on the viability of VHSV-infected FHM cells. FHM cells were seeded into a 96 well plate (SPL life sciences, Korea) with each well containing ~1×10^3 cells. Cells were incubated at 20 °C for 24 h to achieve approximately 80% visual confluency (10 × 10 power, Leica Microsystems, Germany) and then transiently transfected with 1 μg of each engineered pcDNA™3.1(+)*/SsVip* or empty pcDNA™3.1(+), with un-transfected FHM cells used as control. Wells were treated with 1.0, 1.2, 1.4, 1.6, 1.8, 2.0, 2.2, 2.4, and 2.6 of MOI VHSV dilutions 24 h p.t, and incubated at 20 °C for 72 h. Next, the supernatant of the each well was removed by aspiration, 50 μL of 2 mg/mL of freshly prepared 3-(4, 5-dimethylthiazol-2-yl)-2, 5-diphenyltetrazolium bromide (MTT, diluted in PBS) (Sigma) was added, and the cells were incubated at 20 °C for 4 h. After removal of the supernatant by aspiration, 50 μL of dimethyl sulfoxide (DMSO, Sigma) was added. Absorbance at 540 nm was determined using a micro plate reader (MULTISKAN Sky, Thermoscientific).

To confirm the attenuation of virus replication by SsVip, VHSV titers following exposure to SsVip were quantified. Cells were seeded in a 6-well plate (SPL life sciences, Korea), with each well containing ~2×10^3 cells. When the cells reached visual confluency of ~80 (10 × 10 power, Leica Microsystems, Germany), they were transiently transfected with either SsVip/pcDNA™3.1)+ or pcDNA™3.1(+. Twenty four hours after the transfection cells were treated with 1 MOI

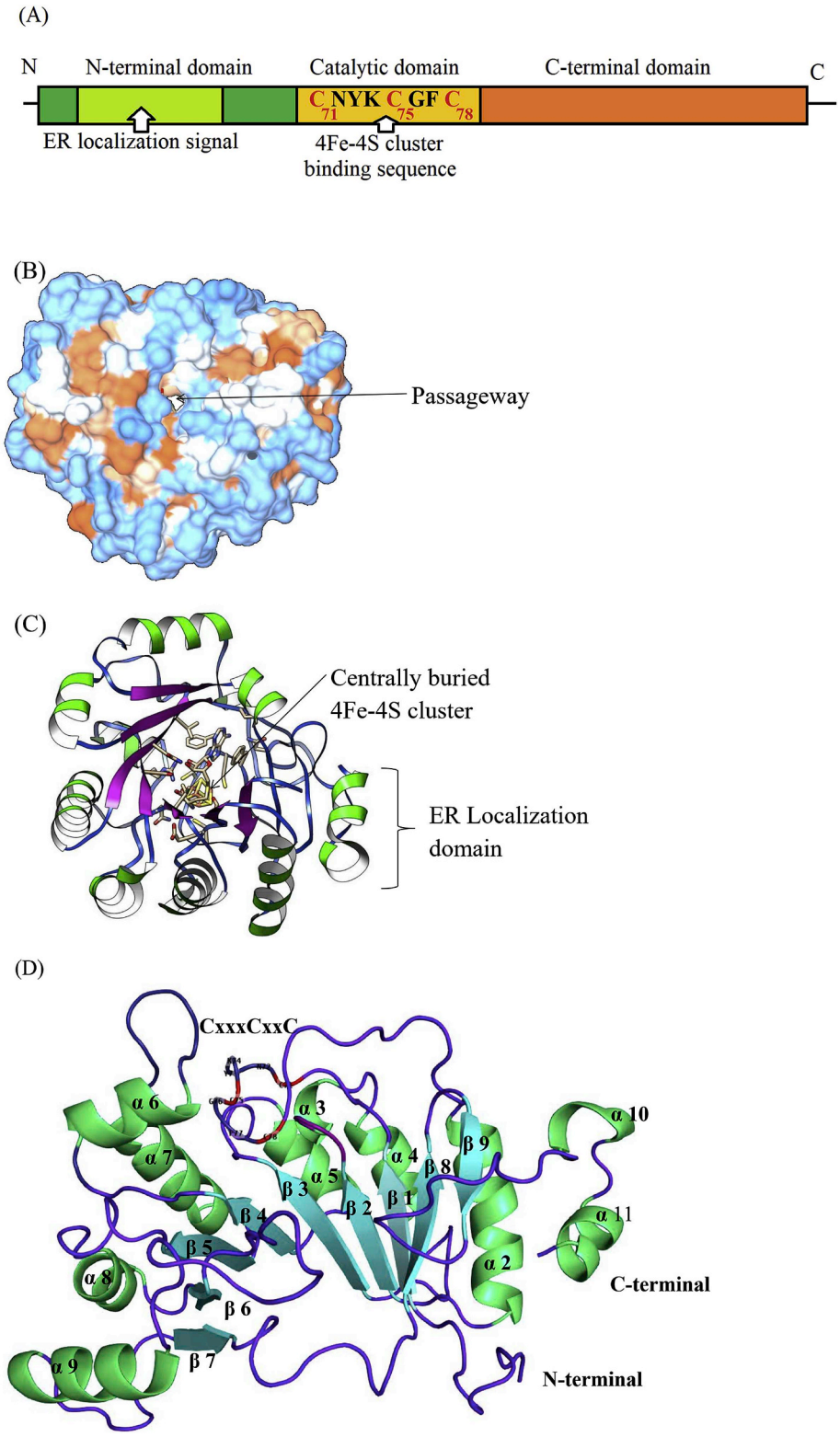

Fig. 1. The structure of SsVip (A) Schematic representation of SsVip's secondary structure, which contains three main domains, namely an N-terminal domain, catalytic domain, and C-terminal domain. The N-terminal domain contains an ER localization signal sequence. A characteristic 4Fe–4S binding site was located in the catalytic domain. Three iron-binding Cys residues (red color) were located at positions 71, 75, and 78. (B) Surface charge distribution of SsVip, wherein red −10, white 0, blue +10. Surface mapping revealed two potential passageways through which reactant and product trafficking is believed to exist between the interior and the exterior of the protein (only one of two passageways is shown here). (C) Homology model of SsVip showing the 4Fe–4S cluster. The radical center depicted in the middle is surrounded by an array of β sheets and α helixes, separating and protecting it from the external environment. (D) Homology model of SsVip displaying the spatial arrangement of secondary structural element. This model consists of eleven α helices (α helix 1 is not shown) and nine β sheets, which are arranged in two layers. (For interpretation of the references to color in this figure legend, the reader is referred to the Web version of this article.)

of VHSV. Samples were incubated for 3 h at 20 °C, after which the cells were thoroughly washed with L-15 media to remove any unattached virus particles. Then, 2 mL of L-15 supplemented with 10% FBS, 1% penicillin, and 1% streptomycin was added to the samples. After 72 h incubation at 20 °C, virus titers produced in each sample were determined as described by Reed and Muench [46].

2.11. Subcellular localization

To determine subcellular localization, pEGFPN1/*SsVip* or empty pEGFPN1 vectors were transiently transfected as described previously. At 30 h p.t., cells were washed with 1 × PBS and fixed with 4% formaldehyde (Sigma, USA) diluted in PBS. Next, 10 μL of 4′,6-diamidino-

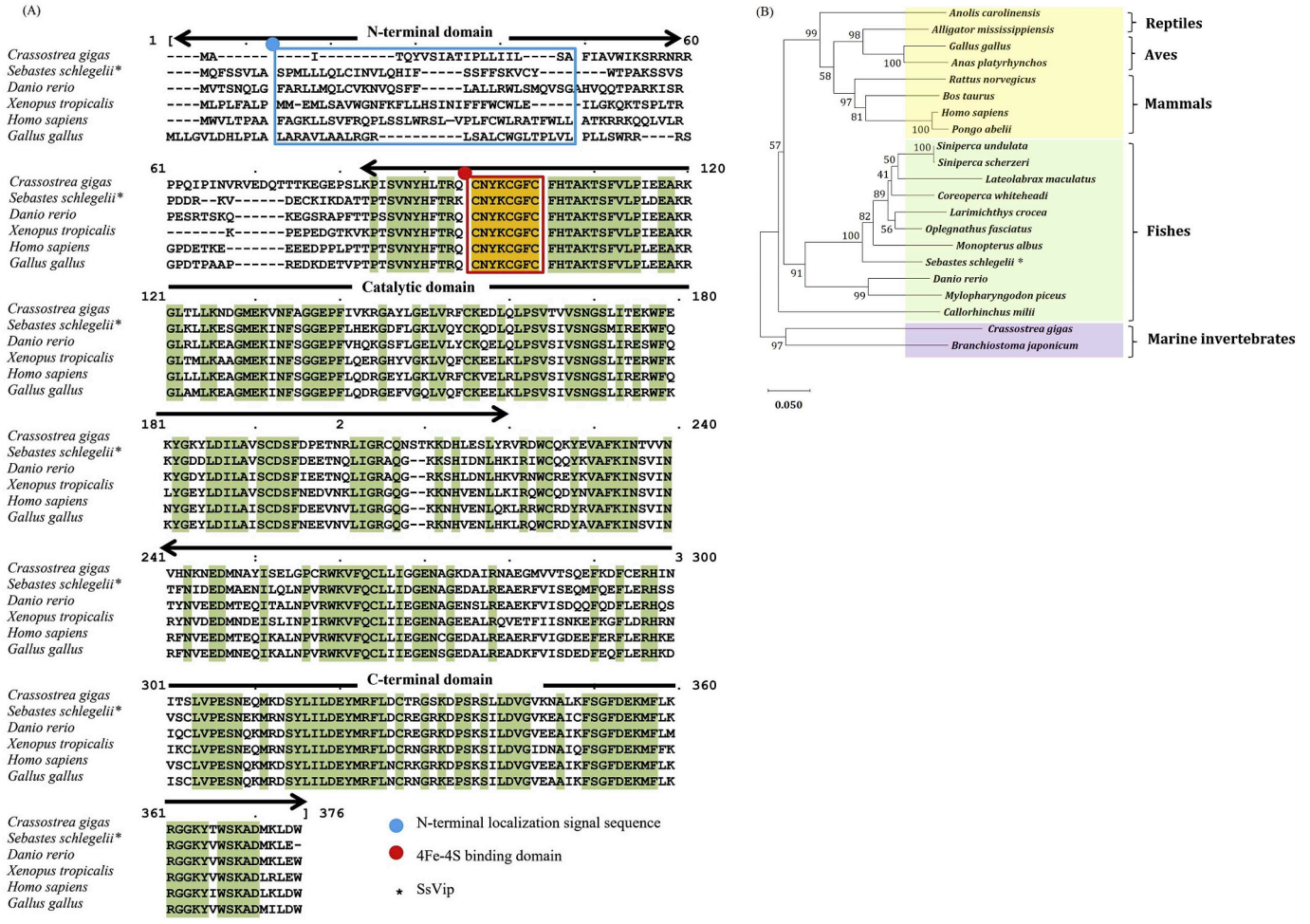

Fig. 2. Sequence comparison and evolutionary relationships of SsVip (A) Multiple sequence alignment of *SsVip* constructed using selected viperin homologues from other vertebrate and invertebrate species. The N terminal ER signal sequence (Blue circle) and characteristic CxxxCxxC motif (Red circle) are shown. (B) Phylogenetic tree of SsVip constructed using vertebrate and invertebrate viperin homologues. This tree was constructed using MEGA (Version 10.0.5) software by using the neighbor-joining method. 5000 bootstrap replicates were performed. The host species and NCBI accession numbers of sequences used for multiple sequence alignment and phylogenetic analysis are as follows: *Branchiostoma japonicum* (ALM30210.1), *Crassostrea gigas* (ALT07791.1), *Gallus gallus* (NP_001305372.1), *Anas platyrhynchos* (AJG06248.1), *Alligator mississippiensis* (KYO32956.1), *Anolis carolinensis* (XP_003215459.1), *Rattus norvegicus* (NP_620236.1), *Bos taurus* (NP_001039406.1), *Homo sapiens* (NP_542388.2), *Pongo abeli* (NP_001129006.1), *Danio rerio* (NP_001020727.1), *Mylopharyngodon piceus* (AQT03380.1), *Siniperca undulata* (ABO48457.1), *Siniperca scherzeri* (ABO48456.1), *Coreoperca whiteheadi* (ABO48449.1), *Larimichthys crocea* (ATO58378.1), *Oplegnathus fasciatus* (AJE63372.1), *Lateolabrax maculatus* (ABO48450.1), *Monopterus albus* (XP_020446533.1), *Callorhinchus milii* (NP_001279633.1) *Xenopus tropicalis* (XP_002935073.1), and *Danio rerio* (NP_001020727.1). The SsVip is indicated by an asterisk (*). (For interpretation of the references to color in this figure legend, the reader is referred to the Web version of this article.)

2-phenylindole (DAPI) (Invitrogen, USA) and 10 μL of ERTracker™ Red dye (Invitrogen, USA) were added. Cell samples were then incubated at 37 °C for 5 h before imaging with a fluorescent microscope (40 × 10 power, Leica Microsystems, Germany). Images were processed by Leica Application Suite X software (Version 3.3).

2.12. Statistical analysis

All experiments were conducted in triplicates. Standard deviation (SD) was used to evaluate the error associated with the measurements. The mean value of three samples was used to contrast the data. Data from the challenge experiment was compared to the control using the Student's t-test, with $p < 0.05$ considered significant. In the MTT assay, cell viability was calculated as previously described (Cell viability = Absorbance of the sample/Absorbance of the control × 100%) [47]. For unchallenged *SsVip* expression, viral RdRp attenuation assay, and MTT assay, significance ($p < 0.05$) was determined using one-way analysis of variance (ANOVA) with Tukey's multiple comparison test.

2.13. Key resources table

Resource	Source	Identifier
Chemical		
3-(4, 5-dimethylthiazol-2-yl)-2, 5-diphenyltetrazolium bromide	Sigma	Cat#M2128
DAPI	Sigma	Cat#D9542
Ampicillin	Sigma	Cat#A0166
DMSO	Sigma	Cat#D2650
formaldehyde	Sigma	Cat#F8775
kanamycin	Sigma	Cat#60615
PBS	Biosesang	Cat#P2007
Penicillin,streptomycin	Thermo Fisher Scientific	Cat#15240062

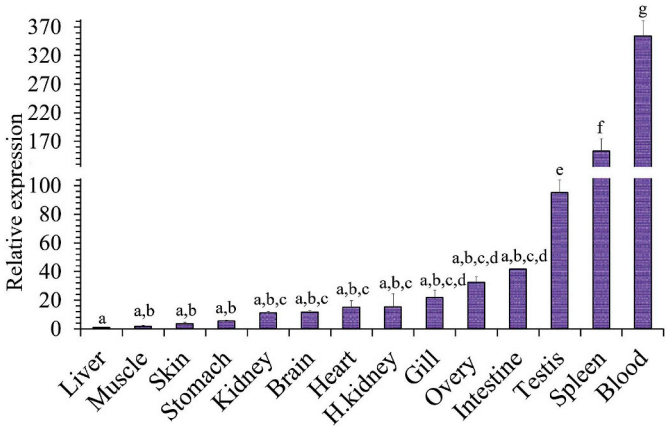

Fig. 3. Transcription profile of *SsVip* under normal physiological conditions by qPCR. Relative *SsVip* mRNA expression was analyzed according to the Livak method. Rockfish *EF1α* was used as the internal control. Data is the mean value of tree replicate experiments and their positive standard deviation (SD). H. kidney is an abbreviated term for head kidney. Data were analyzed with one way ANOVA with Tukey's comparison ($p < 0.05$). Data label with the same lower case letter is not statistically different from each other.

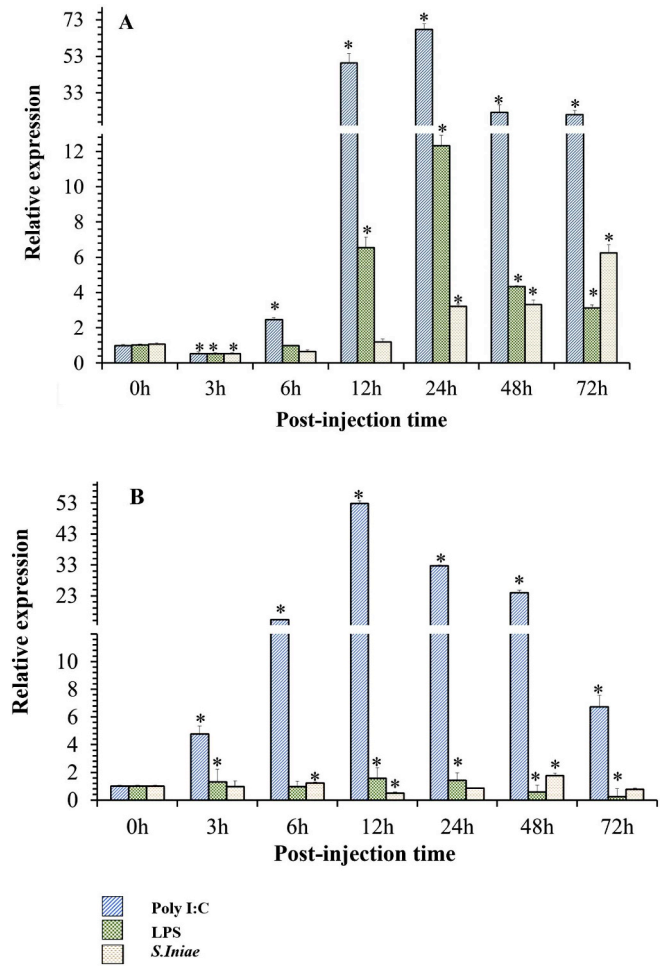

Fig. 4. Relative *SsVip* transcription by qPCR in blood (A) and spleen (B) after the injection of *S. iniae*, poly I:C and LPS. Results for *SsVip* were analyzed according to the Livak method using rockfish *EF1α* as the internal control. Experiments were done in triplicate, mean values and positive standard deviations are shown on the graph. Statistical significance was evaluated with the Student's t-test. Significant values ($p < 0.05$) are indicated with an asterisk (*).

3. Results and discussion

3.1. In silico analysis of SsVip

The length of the *SsVip* open reading frame (ORF) is 1047 bp (Accession No: MK541018). SsVip is a 349 amino acid protein with a calculated size of 40.24 kDa and a pI of 6.67. It contains three main domains (Fig. 1A); an N-terminal ER localization domain, a middle catalytic domain, and a conserved C-terminal domain. The N-Terminal ER localization signal sequence (α1 amphipathic helix) comprises amino acids 9 to 39. A characteristic CxxxCxxC motif (C_{71}NYKC$_{75}$GFC$_{78}$) was observed in residue numbers 71 to 78, which are positioned on a β-barrel fold between β1 and α2. Cys^{71}, Cys^{75}, and Cys^{78} were found to bind with three iron atoms of the 4Fe–4S cluster (Fig. 1A). In previous studies, viperin was classified as a radical SAM enzyme [48], and human viperin was shown to contain a CxxxCxxC motif at position 83 to 90 [49]. In rock bream, the viperin CxxxCxxC motif is positioned between amino acids 76 to 93, and is capable of binding with the 4Fe–4S cluster [29]. Physiochemical studies on this cluster revealed its ability to catalyze a diverse range of radical reactions [50–52]. Therefore, SsVip can be categorized as a radical enzyme capable of catalyzing a wide range of reactions.

Homology modeling of SsVip revealed two passageways positioned on either side of the protein with two openings to the exterior (Fig. 1B). Furthermore, a compact globular structure with a central 4Fe–4S binding CxxxCxxC motif (Fig. 1C) was observed. The CxxxCxxC motif was surrounded by an array of 9 β-sheets and 11 α-helixes, keeping it well-separated from the exterior environment (Fig. 1D). Previous structural studies on seahorse and human viperin revealed them to have a similar globular structure with the reactive center is buried inside the core of the protein [30,48,53]. This conserved structure emphasizes the importance of the reactions SsVip catalyzes. Radical reactions are high energy reactions, involving highly energetic intermediates and products [48]. Therefore, separation of the reactive center from other vital cellular reactions is of paramount importance for proper activity of SsVip.

Pairwise sequence alignment with animal orthologues showed rockfish viperin to have the highest identity (85.2%) and similarity (91.8%) to that of rock bream (Supplementary Table 1), while its identity and similarity to human viperin were 68.4% and 80.6%, respectively. Lower identity (19.7%) and similarity (30.6%) was shown for fruit fly (*Drosophila melanogaster*) viperin. Multiple sequence alignment revealed a number of conserved regions throughout the SsVip (Fig. 2A). Of these, the catalytic domain was found to have the highest sequence conservation. The C-terminal domain also showed a high level of sequence conservation, suggesting probable conserved functions [48]. Similar observations were made regarding the previously characterized seahorse and human viperin C-terminal regions [30,48]. General functions such as dimerization and interaction with partner proteins were allocated to this domain [54–56]. However, no specific antiviral function has been attributed to this region, and more studies are required to functionally characterize the C-terminal domain of the SsVip.

Phylogenetic analysis (Fig. 2B) revealed that SsVip arose separately from other vertebrate groups such as birds, reptiles, and mammals. The clade containing rockfish viperin (⁎) includes other teleosts, namely perch (*Siniperca undulata, Siniperca scherzeri,* and *Coreoperca whiteheadi*), perciforms (*Larimichthys crocea, Oplegnathus fasciatus,* and *Lateolabrax maculatus*) and synbranchiformes (*Monopterus albus*), indicating their close evolutionary relationship with SsVip.

As shown by *in silico* analysis, SsVip is an evolutionary conserved 4Fe–4S cluster-binding, CxxxCxxC motif bearing, radical SAM enzyme.

3.2. Quantitative real time PCR

3.2.1. Tissue distribution of SsVip

Expression analysis with qPCR was performed in order to detect

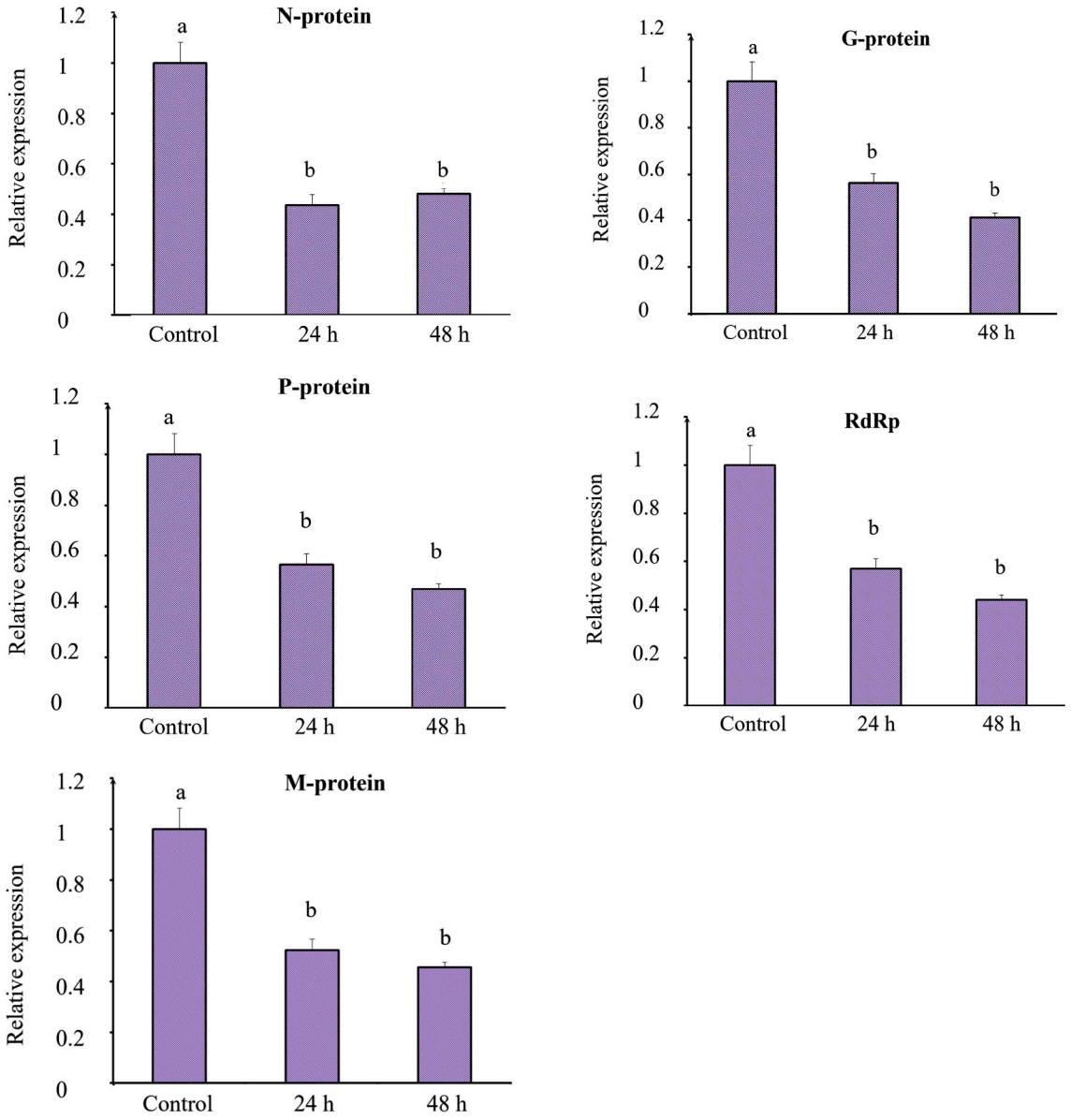

Fig. 5. Downregulation of individual VHSV transcripts accompanying overexpression of SsVip. FHM cells were transfected with pcDNA™3.1(+)/*SsVip* or empty pcDNA™3.1(+) vectors. Cells were treated with 0.01 MOI of VHSV. Samples were collected 24 and 48 h post treatment. Expression of antiviral proteins transcripts was analyzed by qPCR, using *FHMEF1α* as the internal control. Transcription profiles of Nucleoprotein, (*N* protein); Phosphoprotein, (*P* protein); Matrix protein, (*M* protein); Glycoprotein, (*G* protein), and RNA dependent RNA polymerase (*RdRp*) are shown. Each data point represents the mean of three samples; positive SDs are shown. Data was analyzed with one-way ANOVA with Tukey's comparison ($p < 0.05$). Statistical differences are indicated with different lowercase letters.

SsVip under normal physiological conditions, as well as under challenge. The single peak dissociation curve was used as a reference to validate single product amplification during qPCR. At first, expression was monitored to evaluate organ/tissue-specific biases on viperin expression in the absence of significant immune challenge (Fig. 3). The highest expression detected under this condition was in the blood, followed by the spleen and testis. In comparison, the liver, muscle, and skin had the lowest levels of expression.

In a previous study involving rock bream viperin in the absence of immune stimulation, significant upregulation was found in the liver, followed by the spleen, when compared to other organs/tissues [29]. Additionally, two previous studies on red drum and large yellow croaker (*Larimichthys crocea*) viperin found the highest levels of expression to be in blood [25,57]. Blood is a main pathogenic barrier against an array of viruses [58]. Therefore, enhanced expression of ISGs, and of viperin, may be expected in the blood. Since the spleen is closely associated with the blood, similar levels of elevated viperin are unsurprising. In terms of sexual organs, expression of *SsVip* was significantly higher in testes than in ovaries (Fig. 3). Rockfish are a viviparous fish species [59], and therefore their eggs are well protected inside female body, whereas sperm is not. If not fully protected, sperms may carry harmful viral genetic materials to the fetus, therefore testicular cells like Leydig cells, macrophages, Sertoli cells, and peritubular cells were found to express interferons stimulating ISGs, including viperin, continuously [60,61]. This may explain the higher expression of *SsVip* in rockfish testes compared to ovaries.

Different organs/tissues possess different vulnerabilities to pathogens, which may also depend on the niche of the organism. Therefore, the observed variations in *SsVip* transcription can be regarded as early precaution to protect more vulnerable organs/tissues from viruses.

3.2.2. Immune stimulants for SsVip

To evaluate the effect of immune stimulants on the temporal fluctuation profile of *SsVip*, a time dependent challenge experiment was

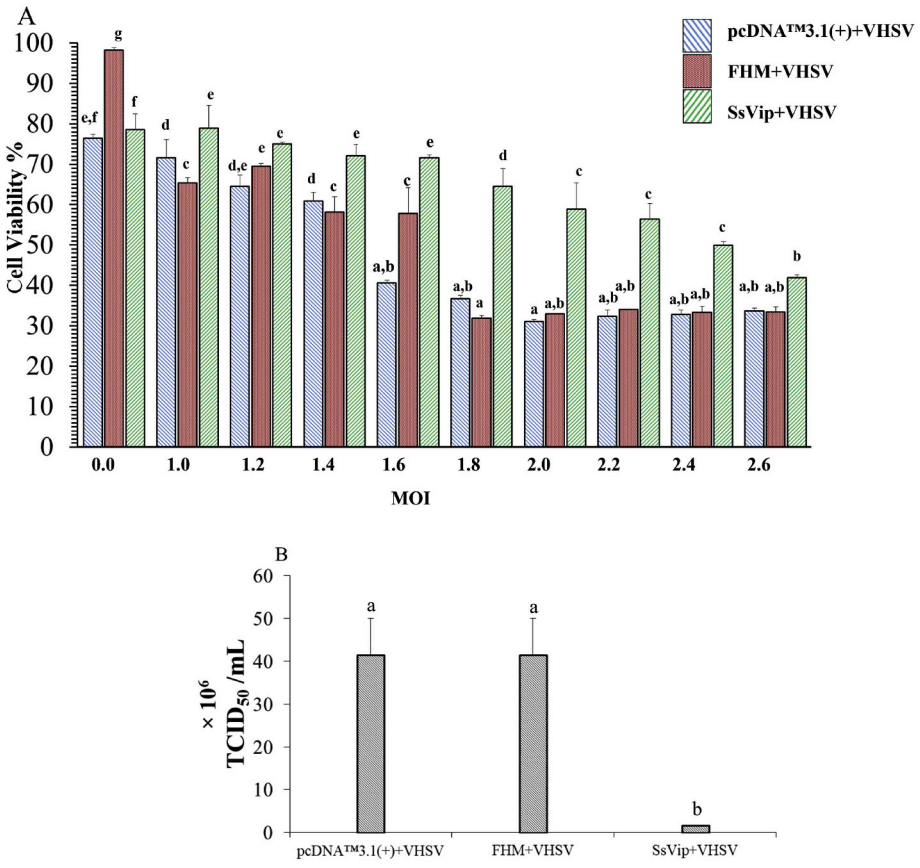

Fig. 6. Cell viability enhancement and VHSV replication attenuation by SsVip. (A) Viability of SsVip transfected FHM cells along with the VHSV MOI. FHM cells were transfected with the pcDNA™3.1(+)/*SsVip* or pcDNA™3.1(+) construct and incubated for 24 h. Cells and FHM were then treated with an increasing MOI titer of VHSV. After 72 h incubation, cell viabilities were analyzed by MTT colorimetric assay. Viability was calculated as a percentage of the control (Un-transfected FHM cells). (B) Reduction of the virus titer with SsVip. The first and second columns represent the virus titers produced by pcDNA™3.1(+) transfected and un-transfected FHM cells, respectively. The third column represents the virus titer produced by the FHM cells transfected with the *SsVip*/pcDNA™3.1 (+) construct. Each data point represents the mean value of three samples and their positive SDs are also shown. Data was analyzed using one-way ANOVA with Tukey's comparison ($p < 0.05$). Statistical differences are indicated with different lowercase letters.

performed. Blood (Fig. 4A) and spleen (Fig. 4B) were selected for this experiment due to the high *SsVip* expression levels observed during the tissue distribution experiment (3.2.1). Results for both spleen and blood revealed a significant and substantial upregulation of *SsVip* following poly I:C stimulation throughout the experiment. Compared to blood, spleen displayed early expression of *SsVip* for poly I:C (Fig. 4A and B). The peak value for blood was reached 24 h post-challenge, while the respective peak for spleen was reached as early as 12 h after challenge. After their respective peak values were reached, expression was observed to gradually decline over time.

Mammalian viperin was rapidly induced upon stimulation with virus and virus-derived materials [62]. Poly I:C is a widely recognized dsRNA analogue which mimics virus-derived dsRNA [63,64]. Studies on marine invertebrates, for example the Pacific oyster (*Crassostrea gigas*), have shown viperin expression to be elevated under poly I:C challenge [65]. In studies among fish, including mandarin fish [26], large yellow croaker [57], red drum [25], and seahorse [30], rapid and marked upregulation of viperin was found following poly I:C stimulation when compared to LPS and other bacterial stimulants. Previous studies performed using poly I:C revealed its ability to activate both dendritic cells (DC) and natural killer (NK) cells through TLR and melanoma differentiation associated receptor (MDA) [66].

The spleen acts as a blood filter, collecting antigens from blood and activating various immune pathways [67]. Splenic DC and macrophages were shown to produce type I and type II IFN upon poly I:C stimulation [63]. Among the ISGs, viperin is a highly expressed gene in animals [4]. Previous studies stated the ability of NK cells to produce IFN-γ for the poly I:C stimulation [66]. Studies have revealed white blood cells (WBC) are highly sensitive for type I and II IFN [68]. Additionally, previous research revealed an inter-organ/tissue correlation for the expression of ISGs [69]. Moreover, lymphocytic choriomeningitis virus (LCMV)-infected mice spleen showed rapid production of type I IFN [70]. Therefore, the spleen is expected to express *SsVip* promptly. However, more time is required for the splenic IFN to act on blood cells, inducing them to express *SsVip*. This type of distinction for ISGs expression might enhance the efficiency of innate immune reactions.

According to our results, viperin expression does not persist over time, and in blood the level of expression gradually decreased after 24 h. In the spleen *SsVip* expression was observed to decline after 12 h. It has been previously demonstrated that cellular IFN expression is transient [71], thus, a decrease in IFN levels could underlie the reduction in *SsVip* expression in blood and spleen.

Besides poly I:C, both LPS and *S. iniae* caused significant upregulation of *SsVip* in blood. When considering LPS, a similar but more moderate *SsVip* expression pattern was observed in blood compared to poly I:C. LPS was used to mimic Gram-negative bacterial endotoxins. In previous analyses, LPS and *S. iniae* caused significant upregulation of viperin in red drum and seahorse [25,30]. LPS was shown to bind to cluster of differentiation 14 receptor (CD14), upregulating type II IFN, and similarly IFN-γ [72]. In a previous study on Atlantic salmon (*Salmo salar*) viperin was found to be upregulated with IFN-γ, but to a lesser degree than type I interferon [73]. Therefore, observed lower expression of *SsVip* in the presence of LPS may be caused by IFN-γ.

Although stimulation of ISGs, including viperin, mainly occurs due to the presence of viruses, bacterial activation by IFN has previously been shown [74]. *S. iniae* is a major Gram-positive pathogenic bacterium [75]. In blood challenged with *S. iniae, SsVip* expression was found to gradually rise. *S. iniae* is reported to either colonize the surface of fish, or to cause an invasive disease [76]. Furthermore, production of IFN-γ in the presence of Gram-negative bacteria such as *Salmonella typhimurium* and Gram-positive bacteria such as *Listeria monocytogenes* has previously been shown [77,78]. Furthermore, TLR-4 mediated endocytosis of bacterial cells followed by IFN-β production has been reported [79]. Recent findings suggest live bacterial phagocytosis as a potential source of mRNA escaping from the phagosomes [80]. This

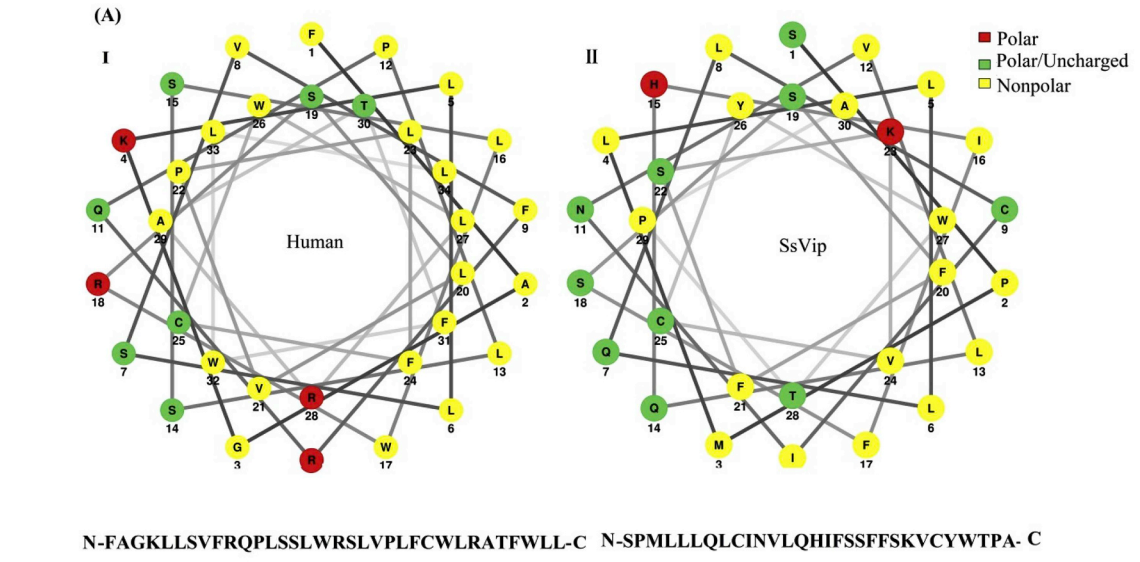

Fig. 7. (A) Helical wheel simulations of human viperin (A-I) and SsVip (A-II) ER localization signals. Both signal sequences are characterized by an abundance of non-polar amino acids. (B) SsVip subcellular localization. FHM cells were transfected with either pEGFPN1/*SsVip* or pEGFPN1. After 24 h cells were inspected with a fluorescent microscope. First lane: FHM cells transfected with pEGFPN1 (control), (I) stained with DAPI (blue); (II) stained with ER tracker™ dye (red); (III) Green fluorescent protein (GFP) (green); (IV) Merged image for I, II, and III. Second lane: pEGFPN1/*SsVip* transfected FHM cell, (V) stained with DAPI (blue); (VI) stained with ER tracker™ dye (red); (VII) SsVip-GFP fusion protein (green); (IX) Merged image of V, VI, and VII. (For interpretation of the references to color in this figure legend, the reader is referred to the Web version of this article.)

escaped bacterial mRNA eventually triggers RIG-1, TLR-3, TLR-7, and MDA-5 receptors, resulting in downstream production of cytokines and expression of ISGs, including viperin [81]. Therefore, the observed upregulation of *SsVip* may have been caused by IFN-β or IFN-γ.

In summary, with the presence of poly I:C, a substantial increase in the expression of *SsVip* was observed in both the spleen and the blood. As previous works suggest, poly I:C is capable of activating multiple pathways leading to the production of both type I and II IFNs. Nevertheless, other immune stimuli such as LPS and *S. iniae* were shown to activate expression of *SsVip* to a lesser degree, mainly through type II IFN (IFN-γ)-producing pathways.

3.3. Virus transcription reduction by SsVip

Significant down regulation of the VHSV gene transcripts for *NP*, *PP*, *MP*, *GP*, and *RdRp* were observed for 24 h and 48 h post-infection samples (Fig. 5). VHSV is a key pathogenic virus in a number of marine and fresh water fishes, including rockfish [82]. The single stranded RNA (ssRNA) genome of VHSV depends solely on RdRp for genome replication, as well as transcription of its genes [83]. Previous studies revealed obligatory sequential transcription of its genes from 3′ end to the 5’ end of the VHSV genome [84]. If RdRp is inhibited by viperin, equal downregulation of all transcripts is expected. To date, no research has been done to evaluate this hypothesis. Therefore, during this research the expression of five VHSV genes were analyzed under conditions of SsVip overexpression. Due to its naturally elevated level compared to other CDS, VHSV *NP* gene expression has been previously used to detect VHSV infections in fishes [85]. A parallel experiment performed using seahorses revealed similar downregulation of VHSV *NP* transcripts [30]. Additionally, human viperin was previously shown to reduce dengue virus transcripts through an RdRp inhibitory mechanism [54]. Both VHSV and dengue virus (DENV) contain ssRNA genomes [54]. Therefore, RdRp can be identified as an obligatory requirement for ssRNA genomic virus transcription. An experiment on oyster viperin revealed its ability to downregulate DENV transcription, moreover, an efficiency comparison between oyster and human viperin revealed similar RdRp inhibitory capacities [86]. According to above findings, viperin has conserved functions against RdRp, whereas the results for SsVip reconfirm previous findings.

3.4. Virus replication reduction by SsVip

The results of the MTT assay for the pcDNA™3.1(+)/*SsVip* transfected cells revealed (Fig. 6A) significant extension of cell viability up to 2.4 MOI. Cells transfected with pcDNA™3.1(+) only showed significant loss of viabilities at VHSV titers exceeding 1.4 MOI. The $TCID_{50}$ values of the SsVip transfected cells (Fig. 6B) showed significant reduction in the virus titers compared to the pcDNA™3.1 + transfected cells and control cells. Cell viabilities of VHSV-infected FHM cells have been previously studied, whereas with VHSV titers of more than 1 MOI, viability losses of approximately sixty percent have been reported [87]. Furthermore, pretreating FHM cells with dsRNA resulted in reduced cell death during VHSV infection through enhanced antiviral effects against VHSV [87]. Such pretreatments would stimulate FHM cells to express ISGs such as viperin at higher concentrations, thereby mounting a cellular antiviral defense against viruses.

Both virus replication and transcription are known to interfere with host cellular activities [88]. Moreover, reduction of cell viability has been shown to be associated with increased VHSV replication levels [89]. The virus quantification assay results confirmed the reduction of virus replication in the presence of SsVip. Therefore, with SsVip overexpression, reduced RdRp activity may have caused for low replication levels of VHSV.

3.5. Subcellular localization of SsVip

Previous research involving carp [28], grouper (*Epinephelus coioides*) [90] and sea horse [30] viperin suggests the cytosolic phase of the ER as the site of viperin localization. Human viperin localization signal (Fig. 7A.I) (NCBI accession number AAL50053, amino acid 9 to 42) was compared to the rockfish localization signal (amino acid 9 to 39) (Fig. 7A.II). Both signal sequences contain a high proportion of non-polar and uncharged amino acids. Moreover, the distribution of polar amino acids is similar in both of these sequences, suggesting that they have similar localization mechanisms.

Findings of this research suggest the ER as the main site of viperin localization (Fig. 7B). Previous findings suggested that the availability of viperin in the cytosolic phase of the ER is important for its antiviral activity, and that it inhibits the trafficking of virus-derived proteins through the ER [7]. Moreover, some viruses are known to use the ER for their replication activity [91], thus by localizing into the ER, SsVip provides cells with additional capability to interfere with virus replication.

4. Conclusion

In this study SsVip was analyzed *in silico*, *in vivo*, and *in vitro*. *In silico* analysis confirmed the availability of the radical iron sulfur binding CxxxCxxC motif at the core of SsVip. *In vivo* immune challenge was designed to evaluate SsVip immune responses, finding it to be drastically upregulated throughout the experiment following challenge with poly I:C. Moreover, low though significant expression of *SsVip* in the presence of non-viral immune stimulants such as LPS and *S. iniae* were observed. An *in vitro* RdRp attenuation assay confirmed previous observations concerning viperin's capacity to enervate viral transcription through RdRp inhibition. An MTT assay and virus titer quantification assay in the presence of SsVip revealed reduction of virus replication. As previous studies have suggested, localization of SsVip to the ER provides cells with additional capacity to directly interfere with virus replication. SsVip is therefore an important antiviral protein in innate immune defense.

Acknowledgments

This research was a part of the project titled 'Fish Vaccine Research Center', funded by the Ministry of Oceans and Fisheries, Korea and supported by Basic Science Research Program through the National Research Foundation of Korea (NRF) funded by the Ministry of Education (2019R1A6A1A03033553).

Appendix A. Supplementary data

Supplementary data to this article can be found online at https://doi.org/10.1016/j.fsi.2019.06.015.

References

[1] S. Baron, F. Dianzani, The interferons: a biological system with therapeutic potential in viral infections, Antivir. Res. 24 (1994) 97–110, https://doi.org/10.1016/0166-3542(94)90058-2.
[2] W.M. Schneider, M.D. Chevillotte, C.M. Rice, Interferon-stimulated genes: a complex web of host defenses, Annu. Rev. Immunol. 32 (2014) 513–545, https://doi.org/10.1146/annurev-immunol-032713-120231.
[3] J.Y.Y. Seo, R. Yaneva, P. Cresswell, Viperin: a multifunctional, interferon-inducible protein that regulates virus replication, Cell Host Microbe 10 (2011) 534–539, https://doi.org/10.1016/j.chom.2011.11.004.
[4] K.S. Duschene, J.B. Broderick, Viperin: a radical response to viral infection, Biomol. Concepts 3 (2012), https://doi.org/10.1515/bmc-2011-0057.
[5] M.T. Nelp, A.P. Young, B.M. Stepanski, V. Bandarian, Human viperin causes radical SAM-dependent elongation of Escherichia coli , hinting at its physiological role, Biochemistry 56 (2017) 3874–3876, https://doi.org/10.1021/acs.biochem.7b00608.
[6] J. Cheek, J.B. Broderick, Adenosylmethionine-dependent iron-sulfur enzymes: versatile clusters in a radical new role, JBIC J. Biol. Inorg. Chem. 6 (2001) 209–226, https://doi.org/10.1007/s007750100210.
[7] E.R. Hinson, P. Cresswell, The N-terminal amphipathic α-helix of viperin mediates localization to the cytosolic face of the endoplasmic reticulum and inhibits protein secretion, J. Biol. Chem. 284 (2009) 4705–4712, https://doi.org/10.1074/jbc.M807261200.
[8] K.J. Helbig, M.R. Beard, The role of viperin in the innate antiviral response, J. Mol. Biol. 426 (2014) 1210–1219, https://doi.org/10.1016/j.jmb.2013.10.019.
[9] Y.M. Loo, M. Gale, Immune signaling by RIG-I-like receptors, Immunity 34 (2011) 680–692, https://doi.org/10.1016/j.immuni.2011.05.003.
[10] K.H. Van der Hoek, N.S. Eyre, B. Shue, O. Khantisitthiporn, K. Glab-Ampi, J.M. Carr, M.J. Gartner, L.A. Jolly, P.Q. Thomas, F. Adikusuma, T. Jankovic-Karasoulos, C.T. Roberts, K.J. Helbig, M.R. Beard, Viperin is an important host restriction factor in control of Zika virus infection, Sci. Rep. 7 (2017) 4475, https://doi.org/10.1038/s41598-017-04138-1.
[11] K.T. Chow, M. Gale, Y.M. Loo, RIG-I and other RNA sensors in antiviral immunity, Annu. Rev. Immunol. 36 (2018) 667–694, https://doi.org/10.1146/annurev-immunol-042617-053309.
[12] J.S. Hee, P. Cresswell, Viperin interaction with mitochondrial antiviral signaling protein (MAVS) limits viperin-mediated inhibition of the interferon response in macrophages, PLoS One 12 (2017) e0172236, , https://doi.org/10.1371/journal.pone.0172236.
[13] A. Stirnweiss, A. Ksienzyk, K. Klages, U. Rand, M. Grashoff, H. Hauser, A. Kroger, IFN regulatory factor-1 bypasses IFN-mediated antiviral effects through viperin gene induction, J. Immunol. 184 (2010) 5179–5185, https://doi.org/10.4049/jimmunol.0902264.
[14] K. Minton, Viperin breaks viral chains, Nat. Rev. Immunol. 18 (2018) 480–481, https://doi.org/10.1038/s41577-018-0035-1.
[15] X. Wang, E.R. Hinson, P. Cresswell, The interferon-inducible protein viperin inhibits influenza virus release by perturbing lipid rafts, Cell Host Microbe 2 (2007) 96–105, https://doi.org/10.1016/j.chom.2007.06.009.
[16] K. Vonderstein, E. Nilsson, P. Hubel, L. Nygård Skalman, A. Upadhyay, J. Pasto, A. Pichlmair, R. Lundmark, A.K. Överby, Viperin targets flavivirus virulence by inducing assembly of noninfectious capsid particles, J. Virol. 92 (2017), https://doi.org/10.1128/JVI.01751-17 e01751-17.
[17] T. Suzuki, Y. Suzuki, Virus infection and lipid rafts, Biol. Pharm. Bull. 29 (2006) 1538–1541, https://doi.org/10.1248/bpb.29.1538.
[18] M.K. Dhar, A. Koul, S. Kaul, Farnesyl pyrophosphate synthase: a key enzyme in isoprenoid biosynthetic pathway and potential molecular target for drug development, N. Biotech. 30 (2013) 114–123, https://doi.org/10.1016/j.nbt.2012.07.001.
[19] P. Mikulecky, E. Andreeva, P. Amara, W. Weissenhorn, Y. Nicolet, P. Macheboeuf, Human viperin catalyzes the modification of GPP and FPP potentially affecting cholesterol synthesis, FEBS Lett. 592 (2018) 199–208, https://doi.org/10.1002/1873-3468.12941.
[20] C. Makins, S. Ghosh, G.D.R. Meléndez, P.A. Malec, R.T. Kennedy, E.N.G. Marsh, Does viperin function as a radical S -Adenosyl-l-methionine-dependent enzyme in regulating farnesylpyrophosphate synthase expression and activity? J. Biol. Chem. 291 (2016) 26806–26815, https://doi.org/10.1074/jbc.M116.751040.
[21] A.S. Gizzi, T.L. Grove, J.J. Arnold, J. Jose, R.K. Jangra, S.J. Garforth, Q. Du, S.M. Cahill, N.G. Dulyaninova, J.D. Love, K. Chandran, A.R. Bresnick, C.E. Cameron, S.C. Almo, A naturally occurring antiviral ribonucleotide encoded by the human genome, Nature 558 (2018) 610–614, https://doi.org/10.1038/s41586-018-0238-4.
[22] H. Zhu, J.P. Cong, T. Shenk, Use of differential display analysis to assess the effect of human cytomegalovirus infection on the accumulation of cellular RNAs: induction

of interferon-responsive RNAs, Proc. Natl. Acad. Sci. 94 (1997) 13985–13990, https://doi.org/10.1073/pnas.94.25.13985.
[23] E.R. Verrier, C. Langevin, A. Benmansour, P. Boudinot, Early antiviral response and virus-induced genes in fish, Dev. Comp. Immunol. 35 (2011) 1204–1214, https://doi.org/10.1016/J.DCI.2011.03.012.
[24] S.H. Lee, K.C. Peng, L.H. Lee, C.Y. Pan, A.L. Hour, G.M. Her, C.F. Hui, J.Y. Chen, Characterization of tilapia (Oreochromis niloticus) viperin expression, and inhibition of bacterial growth and modulation of immune-related gene expression by electrotransfer of viperin DNA into zebrafish muscle, Vet. Immunol. Immunopathol. 151 (2013) 217–228, https://doi.org/10.1016/j.vetimm.2012.11.010.
[25] W. Dang, M. Zhang, Y. Hu, L. Sun, Differential regulation of Sciaenops ocellatus viperin expression by intracellular and extracellular bacterial pathogens, Fish Shellfish Immunol. 29 (2010) 264–270, https://doi.org/10.1016/j.fsi.2010.04.015.
[26] B.J. Sun, P. Nie, Molecular cloning of the viperin gene and its promoter region from the Mandarin fish Siniperca chuatsi, Vet. Immunol. Immunopathol. 101 (2004) 161–170, https://doi.org/10.1016/J.VETIMM.2004.04.013.
[27] B. Sun, I. Skjaeveland, T. Svingerud, J. Zou, J. Jorgensen, B. Robertsen, Antiviral activity of salmonid gamma interferon against infectious pancreatic necrosis virus and salmonid alphavirus and its dependency on type I interferon, J. Virol. 85 (2011) 9188–9198, https://doi.org/10.1128/JVI.00319-11.
[28] B. Wang, Y.B. Zhang, T.K. Liu, J.F. Gui, Sequence analysis and subcellular localization of crucian carp Carassius auratus viperin, Fish Shellfish Immunol. 39 (2014) 168–177, https://doi.org/10.1016/j.fsi.2014.04.025.
[29] B. Zhang, J. Zhang, Z. Xiao, L. Sun, Rock bream (Oplegnathus fasciatus) viperin is a virus-responsive protein that modulates innate immunity and promotes resistance against megalocytivirus infection, Dev. Comp. Immunol. 45 (2014) 35–42, https://doi.org/10.1016/j.dci.2014.02.001.
[30] M.D.N. Tharuka, T.T. Priyathilaka, H. Yang, A. Pavithiran, J. Lee, Molecular and transcriptional insights into viperin protein from Big-belly seahorse (Hippocampus abdominalis), and its potential antiviral role, Fish Shellfish Immunol. 86 (2019) 599–607, https://doi.org/10.1016/j.fsi.2018.12.006.
[31] R.M. Mizanur, S.C. Bai, The optimum feeding frequency in growing Korean rockfish (Sebastes schlegeli) rearing at the temperature of 15°C and 19°C, Australas. J. Anim. Sci. 27 (2014) 1319–1327 https://doi.org/10.5713/ajas.2014.14193.
[32] S. Il Park, Disease control in Korean aquaculture, Fish Pathol. 44 (2009) 19–23, https://doi.org/10.3147/jsfp.44.19.
[33] X. Liu, N. Chen, X. Gao, Y. Zhang, X. Li, Y. Zhang, X. Bing, H. Huang, X. Zhang, The infection of red seabream iridovirus in Mandarin fish (Siniperca chuatsi) and the host immune related gene expression profiles, Fish Shellfish Immunol. 74 (2018) 474–484, https://doi.org/10.1016/J.FSI.2018.01.020.
[34] W.S. Thulasitha, N. Umasuthan, R.G.P.T. Jayasooriya, J.K. Noh, H.C. Park, J. Lee, A thioredoxin domain-containing protein 12 from black rockfish Sebastes schlegelii : responses to immune challenges and protection from apoptosis against oxidative stress, Comp. Biochem. Physiol. C Toxicol. Pharmacol. 185–186 (2016) 29–37, https://doi.org/10.1016/j.cbpc.2016.02.005.
[35] S.F. Altschul, W. Gish, W. Miller, E.W. Myers, D.J. Lipman, Basic local alignment search tool, J. Mol. Biol. 215 (1990) 403–410, https://doi.org/10.1016/S0022-2836(05)80360-2.
[36] K. Okonechnikov, O. Golosova, M. Fursov, Unipro UGENE: a unified bioinformatics toolkit, Bioinformatics 28 (2012) 1166–1167, https://doi.org/10.1093/bioinformatics/bts091.
[37] P. Artimo, M. Jonnalagedda, K. Arnold, D. Baratin, G. Csardi, E. de Castro, S. Duvaud, V. Flegel, A. Fortier, E. Gasteiger, A. Grosdidier, C. Hernandez, V. Ioannidis, D. Kuznetsov, R. Liechti, S. Moretti, K. Mostaguir, N. Redaschi, G. Rossier, I. Xenarios, H. Stockinger, ExPASy: SIB bioinformatics resource portal, Nucleic Acids Res. 40 (2012) W597–W603, https://doi.org/10.1093/nar/gks400.
[38] F. Sievers, A. Wilm, D. Dineen, T.J. Gibson, K. Karplus, W. Li, R. Lopez, H. McWilliam, M. Remmert, J. Soding, J.D. Thompson, D.G. Higgins, Fast, scalable generation of high-quality protein multiple sequence alignments using clustal omega, Mol. Syst. Biol. 7 (2014), https://doi.org/10.1038/msb.2011.75 539–539.
[39] P. Rice, I. Longden, A. Bleasby, EMBOSS: the European molecular biology open software suite, Trends Genet. 16 (2000) 276–277, https://doi.org/10.1016/S0168-9525(00)02024-2.
[40] A. Waterhouse, M. Bertoni, S. Bienert, G. Studer, G. Tauriello, R. Gumienny, F.T. Heer, T.A.P. de Beer, C. Rempfer, L. Bordoli, R. Lepore, T. Schwede, SWISS-MODEL: homology modelling of protein structures and complexes, Nucleic Acids Res. 46 (2018) W296–W303, https://doi.org/10.1093/nar/gky427.
[41] E.F. Pettersen, T.D. Goddard, C.C. Huang, G.S. Couch, D.M. Greenblatt, E.C. Meng, T.E. Ferrin, UCSF Chimera-A visualization system for exploratory research and analysis, J. Comput. Chem. 25 (2004) 1605–1612, https://doi.org/10.1002/jcc.20084.
[42] S. Kumar, G. Stecher, M. Li, C. Knyaz, K. Tamura, MEGA X: molecular evolutionary genetics analysis across computing platforms, Mol. Biol. Evol. 35 (2018) 1547–1549, https://doi.org/10.1093/molbev/msy096.
[43] T.T. Priyathilaka, S.D.N.K. Bathige, S. Lee, J. Lee, Molecular identification and functional analysis of two variants of myeloid differentiation factor 88 (MyD88) from disk abalone (Haliotis discus discus), Dev. Comp. Immunol. 79 (2018) 113–127, https://doi.org/10.1016/j.dci.2017.10.010.
[44] S.A. Bustin, V. Benes, J.A. Garson, J. Hellemans, J. Huggett, M. Kubista, R. Mueller, T. Nolan, M.W. Pfaffl, G.L. Shipley, J. Vandesompele, C.T. Wittwer, The MIQE guidelines: minimum information for publication of quantitative real-time PCR experiments, Clin. Chem. 55 (2009) 611–622, https://doi.org/10.1373/clinchem.2008.112797.
[45] K.J. Livak, T.D. Schmittgen, Analysis of relative gene expression data using real-time quantitative PCR and the $2-\Delta\Delta CT$ method, Methods 25 (2001) 402–408, https://doi.org/10.1006/meth.2001.1262.
[46] L.J. reed, H. Muench, A simple method of estimating fifty per cent endpoints, Am. J. Epidemiol. 27 (1938) 493–497, https://doi.org/10.1093/oxfordjournals.aje.a118408.
[47] D. Fischer, Y. Li, B. Ahlemeyer, J. Krieglstein, T. Kissel, In vitro cytotoxicity testing of polycations: influence of polymer structure on cell viability and hemolysis, Biomaterials 24 (2003) 1121–1131, https://doi.org/10.1016/S0142-9612(02)00445-3.
[48] M.K. Fenwick, Y. Li, P. Cresswell, Y. Modis, S.E. Ealick, Structural studies of viperin, an antiviral radical SAM enzyme, Proc. Natl. Acad. Sci. (2017), https://doi.org/10.1073/pnas.1705402114 201705402.
[49] K.C. Chin, P. Cresswell, Viperin (cig5), an IFN-inducible antiviral protein directly induced by human cytomegalovirus, Proc. Natl. Acad. Sci. Unit. States Am. 98 (2001) 15125–15130 https://doi.org/10.1073/pnas.011593298.
[50] V. Svetlitchnyi, H. Dobbek, W.M. Klaucke, T. Meins, B. Thiele, P. Römer, R. Huber, O. Meyer, A functional Ni-Ni-[4Fe-4S] cluster in the monomeric acetyl-CoA synthase from Carboxydothermus hydrogenoformans, Proc. Natl. Acad. Sci. Unit. States Am. 101 (2004) 446–451 https://doi.org/10.1073/pnas.0304262101.
[51] E.C. Duin, M.E. Lafferty, B.R. Crouse, R.M. Allen, I. Sanyal, D.H. Flint, M.K. Johnson, [2Fe-2S] to [4Fe-4S] cluster conversion in Escherichia coli biotin synthase, Biochemistry 36 (1997) 11811–11820, https://doi.org/10.1021/bi9706430.
[52] H. Hirling, B.R. Henderson, L.C. Kühn, Mutational analysis of the [4Fe-4S]-cluster converting iron regulatory factor from its RNA-binding form to cytoplasmic aconitase, EMBO J. 13 (1994) 453–461, https://doi.org/10.1002/j.1460-2075.1994.tb06280.x.
[53] M. Lei, H. Liu, S. Liu, Y. Zhang, S. Zhang, Identification and functional characterization of viperin of amphioxus Branchiostoma japonicum: implications for ancient origin of viperin-mediated antiviral response, Dev. Comp. Immunol. 53 (2015) 293–302, https://doi.org/10.1016/J.DCI.2015.07.008.
[54] K.J. Helbig, J.M. Carr, J.K. Calvert, S. Wati, J.N. Clarke, N.S. Eyre, S.K. Narayana, G.N. Fiches, E.M. McCartney, M.R. Beard, Viperin is induced following dengue virus type-2 (DENV-2) infection and has anti-viral actions requiring the C-terminal end of viperin, PLoS Neglected Trop. Dis. 7 (2013) e2178, , https://doi.org/10.1371/journal.pntd.0002178.
[55] D. Jiang, H. Guo, C. Xu, J. Chang, B. Gu, L. Wang, T.M. Block, J.T. Guo, Identification of three interferon-inducible cellular enzymes that inhibit the replication of hepatitis C virus, J. Virol. 82 (2008) 1665–1678, https://doi.org/10.1128/JVI.02113-07.
[56] S. Wang, X. Wu, T. Pan, W. Song, Y. Wang, F. Zhang, Z. Yuan, Viperin inhibits hepatitis C virus replication by interfering with binding of NS5A to host protein hVAP-33, J. Gen. Virol. 93 (2012) 83–92, https://doi.org/10.1099/vir.0.033860-0.
[57] J. Zhang, C. Liu, S. Zhao, S. Guo, B. Shen, Molecular characterization and expression analyses of the Viperin gene in Larimichthys crocea (Family: sciaenidae), Dev. Comp. Immunol. 79 (2018) 59–66, https://doi.org/10.1016/j.dci.2017.10.013.
[58] R.A. Goldsby, T.J. Kindt, B.A. Osborne, J. Kuby, Immunology, fifth ed., H. Freeman, New York, NY 10017, US, 2002.
[59] J.P. Wourms, Reproduction and development ofSebastes in the context of the evolution of piscine viviparity, Environ. Biol. Fish. 30 (1991) 111–126, https://doi.org/10.1007/BF02296882.
[60] N. Dejucq, M.O. Lienard, E. Guillaume, I. Dorval, B. Jégou, Expression of interferons-α and -γ in testicular interstitial tissue and spermatogonia of the rat 1, Endocrinology 139 (1998) 3081–3087, https://doi.org/10.1210/endo.139.7.6083.
[61] A. Le Tortorec, H. Denis, A.P. Satie, J.J. Patard, A. Ruffault, B. Jegou, N. Dejucq-Rainsford, Antiviral responses of human Leydig cells to mumps virus infection or poly I:C stimulation, Hum. Reprod. 23 (2008) 2095–2103, https://doi.org/10.1093/humrep/den207.
[62] K.J. Helbig, D.T.Y. Lau, L. Semendric, H.A.J. Harley, M.R. Beard, Analysis of ISG expression in chronic hepatitis C identifies viperin as a potential antiviral effector, Hepatology 42 (2005) 702–710, https://doi.org/10.1002/hep.20844.
[63] S. Trapp, N.R. Derby, R. Singer, A. Shaw, V.G. Williams, S.G. Turville, J.W. Bess, J.D. Lifson, M. Robbiani, Double-stranded RNA analog poly(I:C) inhibits human immunodeficiency virus amplification in dendritic cells via type I interferon-mediated activation of APOBEC3G, J. Virol. 83 (2009) 884–895, https://doi.org/10.1128/JVI.00023-08.
[64] Z. Zhong, Y. Ji, Y. Fu, B. Liu, Q. Zhu, Molecular characterization and expression analysis of the duck viperin gene, Gene 570 (2015) 100–107, https://doi.org/10.1016/J.GENE.2015.06.003.
[65] K.J. Helbig, T.J. Green, D. Raftos, P. Speck, M.R. Beard, L. Geng, Oyster viperin retains direct antiviral activity and its transcription occurs via a signalling pathway involving a heat-stable haemolymph protein, J. Gen. Virol. 96 (2015) 3587–3597, https://doi.org/10.1099/jgv.0.000300.
[66] T. Miyake, Y. Kumagai, H. Kato, Z. Guo, K. Matsushita, T. Satoh, T. Kawagoe, H. Kumar, M.H. Jang, T. Kawai, T. Tani, O. Takeuchi, S. Akira, Poly I:C-induced activation of NK cells by CD8 + dendritic cells via the IPS-1 and TRIF-dependent pathways, J. Immunol. 183 (2009) 2522–2528, https://doi.org/10.4049/jimmunol.0901500.
[67] V. Bronte, M.J. Pittet, The spleen in local and systemic regulation of immunity, Immunity 39 (2013) 806–818, https://doi.org/10.1016/j.immuni.2013.10.010.
[68] L. Xin, D.A.V. Inchaustegui, S.S. Raimer, B.C. Kelly, J. Hu, L. Zhu, J. Sun, L. Soong, Type I IFN receptor regulates neutrophil functions and innate immunity to leishmania parasites, J. Immunol. 184 (2010) 7047–7056, https://doi.org/10.4049/jimmunol.0903273.
[69] Z. Su, M.M. Stevenson, Central role of endogenous gamma interferon in protective immunity against blood-stage plasmodium chabaudi AS infection, Infect. Immun. 68 (2000) 4399–4406, https://doi.org/10.1128/IAI.68.8.4399-4406.2000.
[70] L.N. Lee, S. Burke, M. Montoya, P. Borrow, Multiple mechanisms contribute to

impairment of type 1 interferon production during chronic lymphocytic choriomeningitis virus infection of mice, J. Immunol. 182 (2009) 7178–7189, https://doi.org/10.4049/jimmunol.0802526.
[71] J.H. Colle, C. Carrat, B. Charley, S. Riffault, G. Milon, Transient IFN-γ synthesis in the lymph node draining a dermal site loaded with UV-irradiated herpes simplex virus type 1: an NK- and CD3-dependent process regulated by IL-12 but not by IFN-α/β, J. Gen. Virol. 81 (2000) 2365–2373, https://doi.org/10.1099/0022-1317-81-10-2365.
[72] J.Y. Lee, K.E. Sullivan, Gamma interferon and lipopolysaccharide interact at the level of transcription to induce tumor necrosis factor Alpha expression, Infect. Immun. 69 (2001) 2847–2852, https://doi.org/10.1128/IAI.69.5.2847-2852.2001.
[73] B. Sun, I. Skjæveland, T. Svingerud, J. Zou, J. Jørgensen, B. Robertsen, I. Skjaeveland, T. Svingerud, J. Zou, J. Jorgensen, B. Robertsen, Antiviral activity of salmonid gamma interferon against infectious pancreatic necrosis virus and salmonid alphavirus and its dependency on type I interferon, J. Virol. 85 (2011) 9188–9198, https://doi.org/10.1128/JVI.00319-11.
[74] P. Kovarik, V. Castiglia, M. Ivin, F. Ebner, Type I interferons in bacterial infections: a balancing act, Front. Immunol. 7 (2016) 652, https://doi.org/10.3389/fimmu.2016.00652.
[75] R.P. Perera, S.K. Johnson, M.D. Collins, D.H. Lewis, Streptococcus iniae Associated with Mortality of Tilapia nilotica × T. aurea hybrids, J. Aquat. Anim. Health 6 (1994) 335–340, https://doi.org/10.1577/1548-8667(1994)006<0335:SIAWMO>2.3.CO;2.
[76] M.R. Weinstein, M. Litt, D.A. Kertesz, P. Wyper, D. Rose, M. Coulter, A. McGeer, R. Facklam, C. Ostach, B.M. Willey, A. Borczyk, D.E. Low, Invasive infections due to a fish pathogen, Streptococcus iniae, N. Engl. J. Med. 337 (1997) 589–594, https://doi.org/10.1056/NEJM199708283370902.
[77] E. Berntman, J. Rolf, C. Johansson, P. Anderson, S.L. Cardell, The role of CD1d-restricted NK T lymphocytes in the immune response to oral infection with Salmonella typhimurium, Eur. J. Immunol. 35 (2005) 2100–2109, https://doi.org/10.1002/eji.200425846.
[78] K. Kubota, Y. Kadoya, Innate IFN-γ-producing cells in the spleen of mice early after Listeria monocytogenes infection: importance of microenvironment of the cells involved in the production of innate IFN-γ, Front. Immunol. 2 (2011) 26, https://doi.org/10.3389/fimmu.2011.00026.
[79] D.M. Underhill, H.S. Goodridge, Information processing during phagocytosis, Nat. Rev. Immunol. 12 (2012) 492–502, https://doi.org/10.1038/nri3244.
[80] L.E. Sander, M.J. Davis, M.V. Boekschoten, D. Amsen, C.C. Dascher, B. Ryffel, J.A. Swanson, M. Müller, J.M. Blander, Detection of prokaryotic mRNA signifies microbial viability and promotes immunity, Nature 474 (2011) 385–389, https://doi.org/10.1038/nature10072.
[81] N. Chen, P. Xia, S. Li, T. Zhang, T.T. Wang, J. Zhu, RNA sensors of the innate immune system and their detection of pathogens, IUBMB Life 69 (2017) 297–304, https://doi.org/10.1002/iub.1625.
[82] T. Isshiki, T. Nagano, T. Miyazaki, Susceptibility of various marine fish species to viral hemorrhagic septicemia virus isolated from Japanese flounder, Fish Pathol. 38 (2003) 113–115, https://doi.org/10.3147/jsfp.38.113.
[83] S.H. Kim, S. Yusuff, V.N. Vakharia, Ø. Evensen, Interchange of L polymerase protein between two strains of viral hemorrhagic septicemia virus (VHSV) genotype IV alters temperature sensitivities in vitro, Virus Res. 195 (2015) 203–206, https://doi.org/10.1016/j.virusres.2014.10.013.
[84] S.P. J Whelan, J.N. Barr, G.W. Wertz, Biology of Negative Strand RNA Viruses: the Power of Reverse Genetics, first ed., Springer US, New York, NY 10017, US, 2001.
[85] T. Isshiki, T. Nishizawa, T. Kobayashi, T. Nagano, T. Miyazaki, T. Migazaki, T. Miyazaki, An outbreak of VHSV (viral hemorrhagic septicemia virus) infection in farmed Japanese flounder Paralichthys olivaceus in Japan, Dis. Aquat. Org. 47 (2001) 87–99, https://doi.org/10.3354/dao047087.
[86] T.J. Green, P. Speck, L. Geng, D. Raftos, M.R. Beard, K.J. Helbig, C.J. Timothy Green, Oyster Viperin Retains Direct Antiviral Activity and its Transcription Occurs via a Signalling Pathway Involving a Heat-Stable Haemolymph Protein, (2019), https://doi.org/10.1099/jgv.0.000300.
[87] S.J. Poynter, E.M. Leis, S.J. DeWitte-Orr, In vitro transcribed dsRNA limits viral hemorrhagic septicemia virus (VHSV)-IVb infection in a novel fathead minnow (Pimephales promelas) skin cell line, Fish Shellfish Immunol. 86 (2019) 403–409, https://doi.org/10.1016/j.fsi.2018.11.053.
[88] Q. Ke, W. Weaver, A. Pore, B. Gorgoglione, J.H. Wildschutte, P. Xiao, B.S. Shepherd, A. Spear, K. Malathi, C.A. Stepien, V.N. Vakharia, D.W. Leaman, Role of viral hemorrhagic septicemia virus matrix (M) protein in suppressing host transcription, J. Virol. 91 (2017), https://doi.org/10.1128/JVI.00279-17.
[89] S.H. Kim, B.J. Thu, H.F. Skall, N. Vendramin, O. Evensen, A single amino acid mutation (I1012F) of the RNA polymerase of marine viral hemorrhagic septicemia virus changes in vitro virulence to rainbow trout gill epithelial cells, J. Virol. 88 (2014) 7189–7198, https://doi.org/10.1128/JVI.00423-14.
[90] Y. Zhang, S. Lv, J. Zheng, X. Huang, Y. Huang, Q. Qin, Grouper viperin acts as a crucial antiviral molecule against iridovirus, Fish Shellfish Immunol. 86 (2019) 1026–1034, https://doi.org/10.1016/J.FSI.2018.12.038.
[91] T. Inoue, B. Tsai, How viruses use the endoplasmic reticulum for entry, replication, and assembly, Cold Spring Harb. Perspect. Biol. 5 (2013), https://doi.org/10.1101/cshperspect.a013250 a013250–a013250.